Proceedings of the 28th IEEE
EMBS Annual International Conference
New York City, USA, Aug 30-Sept 3, 2006

Multisite interstitial stimulation for cardiac micro-impedance measurements

Andrew E. Pollard, Roger C. Barr

Abstract— **On theoretical grounds, interstitial current injected and removed using electrodes in close proximity does not cross the membrane, while equilibration of intracellular and interstitial potentials occurs distant from electrodes widely separated. Multisite interstitial stimulation should therefore give rise to interstitial potential differences recorded centrally that depend on intracellular and interstitial micro-impedances, allowing independent measurement. We tested the feasibility of completing such measurements using simulations of multisite stimulation with fine and wide spacing in models that included Luo-Rudy dynamic (LRd) membrane equations. Using two-dimensional models, test data ($\delta\phi_o$) were generated with isotropic interstitial and intracellular micro-impedances prescribed for one set of simulations, and with anisotropic micro-impedances including unequal ratios (intracellular/interstitial) along and across fibers prescribed for another set of simulations. Micro-impedance measurements were then obtained by making statistical comparisons between $\delta\phi_o$ values and interstitial potential differences from passive bidomain simulations ($\triangle\phi_o$) in which a wide range of possible micro-impedances were considered. Our findings suggest development of microfabricated devices to implement the multisite stimulation procedure would facilitate routine measurement as a component of cardiac electrophysiologic study.**

I. Introduction

Mathematical modeling of cardiac electrical activity has provided important insights into mechanisms for arrhythmia initiation, maintenance and termination. Since the presentation of the landmark Luo and Rudy phase II membrane equations in 1994 [1], detailed representations of sarcolemmal currents, ion diffusion, excitation-contraction coupling and intracellular signaling have been systematically integrated into species-, disease- and region-dependent mathematical models for the isolated myocyte. The detail in these membrane equations is a consequence, primarily, of the extensive quantitative data available from single cell electrophysiologic studies. Strategies for careful positioning of myocytes with cellular and subcellular resolution into structural models have also been described. Resulting meshes incorporate details of the cellular architecture available from histologic and imaging data.

Specification of intracellular electrical connections via the myoplasm and gap junctions, and of interstitial connections via the collagenous cleft space remain immature by comparison. Some quantitative detail regarding gap junctional conductance is available from studies using cell pairs that remain attached after disaggregation . In general, however, detail regarding tissue impedances on the size scale of individual myocytes, i.e., cardiac micro-impedances, is unavailable. Because the data is unavailable, investigators who use mathematical modeling often prescribe micro-impedances that allow simulations to replicate indirect measures of tissue status. Micro-impedances prescribed to reflect action potential duration dispersion or conduction velocities do not necessarily reflect those of the tissue.

The discrepancy in detail is a consequence, in large part, of the lack of a straightforward method for micro-impedance measurement that can be integrated into electrophysiologic studies as a routine component. Experiments to obtain this data are technically challenging. They require a sequence of transmembrane potential (V_m) recordings to be made in close proximity to a stimulating electrode to measure the electrotonic decay in V_m from which intracellular and interstitial micro-impedances are derived. The approach is largely impractical for multi-dimensional preparations because accurate positioning of the fragile electrodes is problematic. Furthermore, analytic frameworks for interpreting the V_m decay are closely related to the one-dimensional continuous core-conductor model, so their applicability to tissue preparations is limited.

One possible method to overcome the limitations of these traditional approaches is multisite interstitial stimulation [2]. Stimulation with electrodes separated over a distance that is small with respect to the space constant establishes a central interstitial potential difference that reflects interstitial current flow [3]. Then, stimulation with more widely spaced electrodes establishes a lower interstitial potential difference because the applied current redistributes between interstitial and intracellular compartments. We recently showed that interstitial potential differences during multisite

1-4244-0033-3/06/$20.00 ©2006 IEEE.

stimulation in one-dimensional Luo and Rudy dynamic (LRd) membrane equation [1], [4], [5], [6] simulations could be fit to the analytic response assuming a core-conductor geometry. That fit allowed highly accurate intracellular and interstitial micro-impedance measurements to be obtained. In the present study, we present a new approach that allows use in multi-dimensional preparations. Instead of fitting interstitial potential differences to an analytic response, we make statistical comparisons to interstitial potential differences obtained from passive simulations in which a wide range of possible micro-impedances are considered.

II. Methods

LRd simulations using two-dimensional bidomain models to obtain interstitial potential differences ($\delta\phi_o$) during multisite interstitial stimulation were completed. Individual myocytes within the models included nodes that were separated from one another at fixed space steps of $\triangle$x=$\triangle$y=12.5 μm in arrangements analogous to that shown in the circuit diagram in Figure 1A. With that spacing, 8 individual segments were located along each LRd myocyte of 100 μm length and 2 individual segments were located across myocytes separated laterally by 25 μm. In Figure 1A, the dashed line surrounding the components within the diagram represents the myocyte boundary. Responses to multisite interstitial stimulation were assessed in models in which the intracellular and interstitial micro-impedances in the x and y directions from Figure 1A were assumed to be either isotropic or anisotropic. The isotropic micro-impedances we prescribed were g_{ix}=g_{iy}=1.60 mS/cm and g_{ox}=g_{oy}=2.86 mS/cm. For the anistropic model, we prescribed values of g_{ox}=3.17 mS/cm and g_{ix}=4.82 mS/cm assuming fibers oriented in the x direction of Figure 1A, and values of g_{oy}=1.17 mS/cm and g_{iy}=0.51 mS/cm assuming the y direction was across fibers.

Nodes within each model were identified as recording or stimulation sites to obtain the $\delta\phi_o$ values. Figure 1B shows sites positioned along the x axis. The central recording electrodes (white circles), denoted B and C, were separated from one another by 25 μm to insure that a sufficient number of stimulating electrodes could be positioned within 5 myocytes laid end-to-end. A set of 9 nodes (black circles) located to the left of the B electrode and denoted Ai-Aix were used for interstitial current injection. The separation between the center of the recording pair and each of the current injection electrodes, denoted p, varied from 37.5 μm to 237.5 μm in 25 μm steps. Similarly, a set of current removal electrodes (Di-Dix) were positioned with separation from the center of the recording pair (q) at 37.5 μm to 237.5 μm such that 20 total electrodes made up the fine spacing region in each model. Figure 1C shows sites selected for current injection (Ax-Axv) and removal (Dx-Dxv) in a wide spacing region with 400 μm steps between electrodes. All simulations were completed with the electrodes oriented as shown in Figure 1B and 1C.

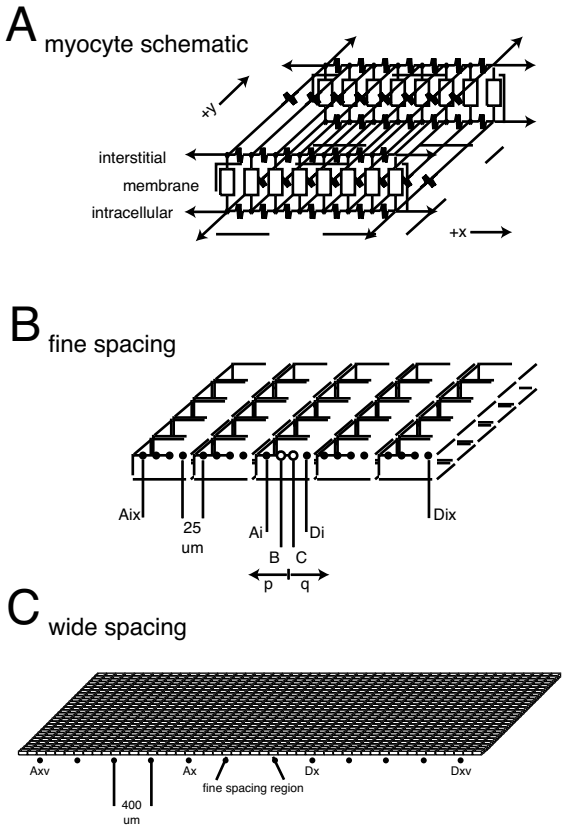

Figure 1

Once $\delta\phi_o$ values were available, we made statistical comparisons to interstitial potential differences from passive bidomain simulations ($\triangle\phi_o$) in which wide ranges of possible micro-impedances were considered. To make these comparisons, we developed a table lookup procedure that we term SCAT because it involves (S) simulations with passive bidomain models, (CA) comparison of alternative micro-impedance choices and (T) tabulation for measurements within defined error bounds. Large numbers of passive bidomain simulations were completed using a constant membrane micro-impedance (R_m in $k\Omega{\cdot}cm^2$) in place of the LRd model current. We emphasize that R_m was not prescribed in the LRd simulations,

but instead resulted from combination of the available sarcolemmal channels during the action potential plateau when interstitial stimuli were applied. Therefore, its intrinsic value was identified as a part of the measurement process. Possible micro-impedances were treated as SCAT table inputs, with $\triangle\phi_o$ using different stimulating electrode combinations treated as SCAT table outputs. To compare alternative micro-impedances, we then calculated the statistical variance (σ^2) between $\triangle\phi_o$ and $\delta\phi_o$ values for each stimulating electrode combination. Differences (Y) were quantified using different stimulating electrode combinations. Tables were then searched to identify entries at which Y was minimized. As $\delta\phi_o$ and $\triangle\phi_o$ values approached one another in table entries, improved matches between SCAT table and prescribed micro-impedances were found.

III. Results

With the isotropic model, we selected the Ai-Di, Aiv-Div and Aix-Dix stimulating electrode combinations for SCAT table assembly in an attempt to resolve the observed decay in $\delta\phi_o$. Once these combinations were selected, we built a SCAT table using 25% adjustments over bounds of 0.056-10.00 mS/cm for g_{ix}, 0.056-10.00 mS/cm for g_{ox}, and 0.50- 49.89 $k\Omega{\cdot}cm^2$ for R_m. This SCAT table included 6,137 entries. Assembly required 426 hours (17.7 days) total computational time. Figure 2A shows Y differences plotted against entry number and grouped by the marked R_m values. The closest available match to the prescribed g_{ix} of 1.60 mS/cm was at 1.78 mS/cm (11.25%), while the closest available match to the prescribed g_{ox} of 2.86 mS/cm was at 2.87 mS/cm (0.34%). These parameters were identified at the lowest Y.

Intracellular and interstitial micro-impedances of comparable accuracy were also obtained with the anisotropic model. For SCAT table analysis, the widest separation we considered was the Ax-Dx stimulating electrode combination. Because SCAT table analysis requires that the number of $\delta\phi_o$ values match or exceed the number of individual micro-impedances, $\delta\phi_o$ with the Ai-Di, Aii-Dii, Aiii-Diii and Av-Dv stimulating electrode combinations were additionally included. Once these combinations were selected, we built a SCAT table with 25% adjustments over bounds of 1.90-4.50 mS/cm for g_{ox}, 2.74-6.50 mS/cm for g_{ix}, 1.12-2.00 mS/cm for g_{oy}, 0.56-1.00 mS/cm for g_{iy}, and 3.00-7.11 $k\Omega{\cdot}cm^2$ for R_m. Generation of the table, which contained 1,024 entries, required 153 hours (6.4 days) computational time. Figure 2B shows all Y plotted against SCAT table entry number. At the lowest overall Y, micro-impedances of g_{ix}=4.88 mS/cm, g_{ox}=3.38 mS/cm, g_{iy}=0.42 mS/cm and g_{oy}=1.12 mS/cm were identified. Therefore, all values were within the 25% steps used for SCAT table assembly.

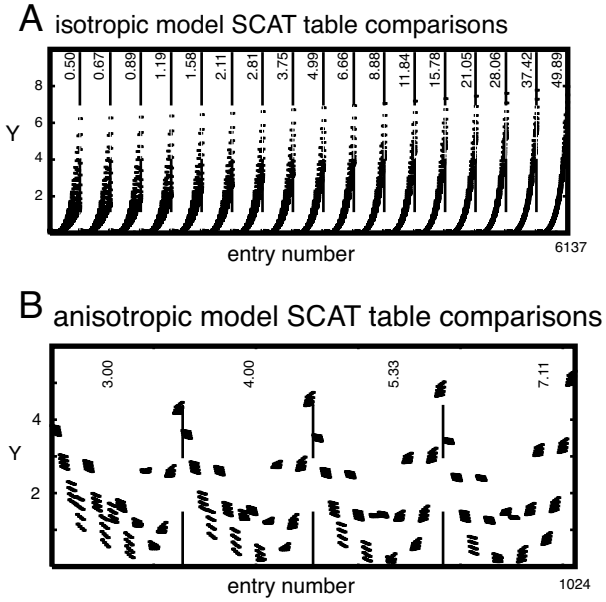

Figure 2

IV. Discussion

The specific aim of the present study was to assess the feasibility of using multisite interstitial stimulation to measure cardiac micro-impedances in two-dimensional preparations. As shown in our earlier report [2] that focused on conditions detailed by Weidmann [7], positioning a set of interstitial stimulating electrodes in close proximity to a central recording pair allowed one set of $\delta\phi_o$ responses to be recorded in which relatively little of the injected current crossed the cell membrane before removal. With wider spacing between the stimulating electrodes, the injected current equilibrated between the intracellular and interstitial volume conductors before removal, resulting in lower $\delta\phi_o$ responses that reflected that redistribution. Assuming a core-conductor geometry then allowed analytic solution for the interstitial potential gradient in terms of the stimulating electrode positions and the intracellular and interstitial micro-impedances. Nonlinear least-squares analyses of $\delta\phi_o$ over a range of stimulating electrode combinations led to highly accurate micro-impedance measurements and quantification of the gap junctional contributions to overall cellular uncoupling. The

present study extends that report significantly. In particular, we removed the restrictive assumption of a core-conductor geometry as part of the measurement process. Replacing that part with the statistical approach allows for arbitrary geometric arrangements, provided $\delta\phi_o$ recordings are made with sufficiently fine spatial resolution and multisite stimulating electrode combinations allow resolution of $\delta\phi_o$ changes with adjustments in those combinations. When these criteria were met, we found that a process of assessing $\delta\phi_o$ to select stimulating electrode combinations for SCAT table assembly and analyzing $\triangle\phi_o$ %-differences allowed accurate micro-impedance measurements.

The general utility of our approach is a consequence of the relatively low computational expense for any one passive simulation. That low expense allows large numbers of micro-impedance combinations to be made available for the statistical comparisons. Furthermore, the addition of entries is straightforward, allowing refinements to the SCAT table when reduction in $\triangle\phi_o$ %-differences is desired. Analyses with SCAT tables, once assembled, are rapid because the process involves table look-up. Development of the SCAT table approach was instrumental in obtaining the accurate micro-impedances measurements in the present study, and we emphasize that the approach has significant advantages over alternative methods. All entries computed for these analyses are available for reuse. This has implications for future experimental studies because assembly of electrode arrangements with dimensions considered here will allow direct use of the SCAT tables built to date. Because the SCAT tables were built from passive bidomain simulations, any adjustments in stimulus current magnitude will simply require scaling of $\triangle\phi_o$ values. In the event that experimental electrode arrangements differ from those we considered, any entries associated with stimulating electrode combinations that we did consider will be available to populate portions of new SCAT tables, limiting the number of combinations required for that population. The process of assembling an initial SCAT table requires minimal information regarding passive simulations that have been or need to be completed. In the event that full retabulation were necessary, the independence of the individual passive simulations suggests determination of SCAT table entries as an excellent candidate for grid computing using 100s or 1000s of processors because no communication overhead would be associated with that tabulation.

Support. U. S. Public Health Service under Grants HL67728 and HL67961.

Affiliations. A.E. Pollard (pollard@crml.uab.edu) is with Biomedical Engineering and the Cardiac Rhythm Management Laboratory at the University of Alabama at Birmingham. Volker Hall/B140, 1670 University Blvd., Birmingham, AL 35294. R.C. Barr (roger.barr@duke.edu) is with Biomedical Engineering at Duke University. Hudson Hall/136, Durham, NC 27708.

References

[1] Luo C-H and Rudy Y, "A dynamic model of the cardiac ventricular action potential. I. Simulations of ionic currents and concentration changes," *Circ. Res.*, vol. 74, pp. 1071–1096, 1994.

[2] Pollard AE, Smith WM, and Barr RC, "Feasibility of cardiac microimpedance measurement using multisite interstitial stimulation," *Am. J. Physiol. Heart Circ. Physiol.*, vol. 287, pp. H2402–H2411, 2004.

[3] Plonsey R and Barr RC, "The four-electrode resistivity technique as applied to cardiac muscle," *IEEE Trans. Biomed. Eng.*, vol. 7, pp. 983–986, 1982.

[4] Hund TJ and Rudy Y, "Determinants of excitability in cardiac myocytes: mechanistic investigation of memory effect," *Biophys. J.*, vol. 79, pp. 3095–3104, 2000.

[5] Hund TJ, Kucera JP, Otani NF, and Rudy Y, "Ionic charge conservation and long-term steady state in the luo-rudy dynamic cell model," *Biophys. J.*, vol. 81, pp. 3324–3331, 2001.

[6] Pollard AE, Cascio WE, Fast VG, and Knisley SB, "Modulation of triggered activity by uncoupling in the ischemic border: A model study with phase 1b-like conditions," *Cardiovasc. Res.*, vol. 56, pp. 381–392, 2002.

[7] Weidmann S, "Electrical constants of trabecular muscle from mammalian heart," *J Physiol*, vol. 210, pp. 1041–1054, 1970.